Carbohydrate Polymers 112 (2014) 440–447

Contents lists available at ScienceDirect

Carbohydrate Polymers

journal homepage: www.elsevier.com/locate/carbpol

Molecular self assembly of mixed comb-like dextran surfactant polymers for SPR virus detection

Katanchalee Mai-ngam[a,*], Wansika Kiatpathomchai[b,c], Narong Arunrut[b,c], Jitlada Sansatsadeekul[a]

[a] National Metal and Materials Technology Center, 114 Thailand Science Park, Paholyothin Rd., Klong 1, Klong Luang, Pathumthani 12120, Thailand
[b] CENTEX Shrimp, Faculty of Science, Mahidol University, Rama 6 Rd., Bangkok 10400, Thailand
[c] National Center for Genetic Engineering and Biotechnology, 113 Thailand Science Park, Paholyothin Rd., Klong 1, Klong Luang, Pathumthani 12120, Thailand

ARTICLE INFO

Article history:
Received 31 March 2014
Received in revised form 19 May 2014
Accepted 3 June 2014
Available online 17 June 2014

Keywords:
Surface plasmon resonance
Dextran surfactant polymer
Virus
Bimodal molecular weight distribution

ABSTRACT

The synthesis of two comb-like dextran surfactant polymers, that are different in their dextran molecular weight (*MW*) distribution and the presence of carboxylic groups, and their characterization are reported. A bimodal carboxylic dextran surfactant polymer consists of poly(vinyl amine) (PVAm) backbone with carboxyl higher *MW* dextran, non-functionalized lower *MW* dextran and hydrophobic hexyl branches; while a monomodal dextran surfactant polymer is PVAm grafted with non-functionalized lower *MW* dextran and hexyl branches. Layer formation of non-covalently attached dextran chains with bimodal *MW* distributions on a surface plasmon resonance (SPR) chip was investigated from the perspective of mixed physisorption of the bimodal and monomodal surfactant polymers. Separation distances between the carboxylic longer dextran side chains within the bimodal surfactant polymer and between the whole bimodal surfactant molecules on the chip surface could be well-controlled. SPR analysis of shrimp yellow head virus using our mixed surfactant chips showed dependence on synergetic adjustment of these separation distances.

1. Introduction

Early disease detection is important to success in disease treatment, management, and control. Another critical advantage is that detection before the symptoms appear may minimize or avoid health and economic impacts associated with the spread of infectious diseases. Surface plasmon reasonance (SPR) biosensors have recently gained considerable attention as an effective means for biomolecular detection and medical diagnostics due to their label-free and high throughput capabilities. In a typical experiment, a ligand is immobilized to a functionalized gold chip surface and an aqueous analyte solution is flown across the surface in order to quantify in real-time the extent of ligand–analyte binding. The binding results in a change of the refractive index on the sensor surface, which can be monitored as a change in resonance angle, resonance wavelength or reflectivity.

Effective coupling of the ligand can improve sensor chip sensitivity, leading to an upsurge in SPR applications (Richens et al., 2009). A variety of SPR sensor chips, previously reported and/or commercially available, can be classified into two groups: self-assembled monolayer-based (2D) and covalently grafted hydrogel-based (3D) chips (Löfås & McWhirter, 2006). The 3D polymeric chips become a more popular choice due to their higher density of immobilized ligand, more stability and solution-like environment for the ligand. However, a planar chip surface generates less steric crowding as compared to a 3D surface. Therefore, it is more preferable for experiments where the binding between two large molecules is measured (Lahiri, Isaacs, Tien, & Whitesides, 1999). New ligand coupling constructs are presented here to address the problem of SPR detection of whole-cell viruses and bacteria, limited mainly due to its low sensitivity (Lei et al., 2008; Puttharugsa et al., 2011).

Non-covalent physisorption, which is mainly achieved by self-assembly of polymeric surfactants on a surface, is a promising modification strategy of hydrophobic biomedical materials

* Corresponding author. Tel.: +66 2 564 6500; fax: +66 2 564 6446.
E-mail addresses: Katanchalee.Mai-ngam@nstda.or.th, kmaingam@gmail.com (K. Mai-ngam), wansika@biotec.or.th (W. Kiatpathomchai), narong.aru@biotec.or.th (N. Arunrut), jitladas@mtec.or.th (J. Sansatsadeekul).

http://dx.doi.org/10.1016/j.carbpol.2014.06.022
0144-8617/

which typically contain no labile functional groups required for covalent immobilizations (Helmus & Hubbell, 1993). Surfactant polymers with different molecular geometries (AB diblock, ABA triblock and comb-like surfactants) have been explored as potential surface-modifying agents with thromboresistant and/or antibacterial properties (Bridgett, Davies, & Denyer, 1992; Holland, Qiu, Ruegsegger, & Marchant, 1998; Mai-ngam, 2006; Marsh et al., 2002; Park, Cho, Kwon, Jeong, & Bae, 2002; Qiu, Zhang, Ruegsegger, & Marchant, 1998; Ruegsegger & Marchant, 2001; Sagnella & Mai-Ngam, 2005; Sen Gupta et al., 2006; Vacheethasanee & Marchant, 2000; Zhu & Marchant, 2006). For biosensor applications, various small molecule surfactants have been used to non-covalently functionalize carbon nanotube electrodes in order to suspend carbon nanotubes in aqueous medium and to couple biomolecules (Bianco et al., 2007). In contrast, this has only been achieved with a few surfactant polymers (Kam, Liu, & Dai, 2005). Moreover, surfactant polymers have not been used to date in SPR biosensor technology.

In this study, we describe the development of bimodal dextran SPR chips for improving sensitivity of whole-cell virus detection. We hypothesized that steric repulsion induced by the long-chain dextran segments more effectively repels relatively large-size viruses away from the chip surface, as compared to small biomolecules, and consequently prevents required ligand–receptor bridging. To control the repulsion, non-covalently 'end-on' attached dextran matrices with bimodal *MW* distributions on a chip surface were prepared by mixed physisorption of bimodal and monomodal surfactant polymers. The bimodal one consists of poly(vinyl amine) (PVAm) backbone with carboxyl higher *MW* dextran, non-functionalized lower *MW* dextran and hydrophobic hexyl pendant groups; while the monomodal one is PVAm grafted with non-functionalized lower *MW* dextran and hexyl branches. We proposed possible models of molecular surface alignment of the mixed surfactant chips and also correlated them to the SPR sensitivity of shrimp yellow head virus (YHV) detection.

2. Experimental

2.1. Materials

Two dextrans, namely dextran 10K and dextran 1.5K, with molecular masses of 10,000 g/mol and 1500 g/mol, respectively, were purchased from Fluka Analytical (Missouri, USA). *N*-hydroxysuccinimide (NHS), 4-(2-hydroxyethyl)-1-piperazineethanesulfonic acid (HEPES), ethylenediaminetetraacetic acid (EDTA), and sodium borohydride were also obtained from Fluka Analytical. *N*-vinyl formamide, 2,2′-azobisisobutyronitrile (AIBN), allyl bromide, hexanoic acid, silver carbonate, 6-mercaptohexadecanoic acid, and Toluidine Blue-O (TBO) were obtained from Sigma-Aldrich Corporation (Missouri, USA). Iodine, sodium chloride, sodium acetate, 1-ethyl-3-(3-dimethylaminopropyl)carbodiimide (EDC), and Tween-20 were provided from Merck (New Jersey, USA). Potassium hydroxide was purchased from Ajax Finechem and 2-morpholinoethane sulfonic acid (MES) was obtained from Acros Organics (Geel, Belgium). Acetic acid was purchased from Labscan (Bangkok, Thailand). Amberlite IR-120 strong cationic exchange resin and Amberlite IR-400 strong anionic exchange resin were purchased from Sigma-Aldrich Corporation and rinsed with deionized (DI) water before use. All other reagents and solvents were used as received unless otherwise specified.

2.2. Methods

Preliminary study of reversible self-assembling of the bimodal and monomodal dextran surfactant polymers has been previously reported briefly, but no characterization data other than contact angle measurement was presented (Sansatsadeekul & Mai-ngam, 2013). In this report, different characterization techniques were employed to better understand the chemical compositions of the surfactant polymers and their self-assembling arrangement on the SPR gold chip surface.

Transmission Fourier transform infrared (FTIR) spectra in the wavelength range of 400–4000 cm^{-1} were obtained using a Perkin Elmer System 2000R FTIR spectrometer (Massachusetts, USA). The materials were ground with KBr and pressed into pellets under vacuum. The spectrum of each sample was then collected from 100 scans with a resolution of 4 cm^{-1}. Proton nuclear magnetic resonance (^1H NMR) spectra were obtained from a 400 MHz Bruker DRX-400 spectrometer (Massachusetts, USA) using D_2O as solvent and an internal reference peak of residual hydroxy at 4.67 parts per million. The elemental analysis of the obtained products was performed using a Leco TruSpec CHN analyzer (Michigan, USA). The estimated analysis of two different elements, carbon and nitrogen, was undertaken.

Gel permeation chromatography (GPC) studies were performed using a Water 600E system controller (Massachusetts, USA) equipped with an Ultrahydrogel linear column and a refractive index detector. All the measurements were carried out at the flow rate of 0.6 mL/min using 0.1 M sodium nitrate buffer (pH 7) as eluent.

The surface active properties of the surfactant polymers in solution at an air/water interface were determined from water surface tension measurements. Surface tensions of aqueous surfactant polymer solutions were measured at 25 °C and ambient pressure, using a Dataphysics DCAT 11 tensiometer (Filderstadt, Germany). Assembly of the surfactant polymers on gold chip surfaces was studied using a SPI-4000 atomic force microscope (AFM) from Seiko Instruments Inc. (Japan) operating in dynamic force mode. Silicon nitride (Si_3N_4) cantilevers with integrated Si_3N_4 tips (SI-DF3, Seiko Instruments Inc.) were used.

2.3. Preparation and matrix layer formation of dextran surfactant polymers

Scheme 1 shows a synthesis route to the bimodal dextran surfactant polymers. PVAm ($M_n \sim 100{,}000$), synthesized according to a method reported previously (Qiu et al., 1998; Sansatsadeekul & Mai-ngam, 2013), was selected as a backbone for all surfactant polymers. For the bimodal carboxyl dextran surfactants, dextran 10K aldonic acid were first attached to PVAm through the standard EDC and NHS activation reaction in a 2-morpholinoethane sulfonic acid (MES) buffer system. After allylation of PVAm-*g*-dextran 10K, dextran 1.5K aldonic acid chains were sequentially attached using the similar reaction. The unreacted amine groups on the backbone were further grafted with hexanoic acid and the allyl groups on the dextran 10K were converted to carboxylic acid. The monomodal surfactant polymer, PVAm with non-functionalized dextran 1.5K and hexyl branches, was synthesized and characterized using similar procedures, except with the absence of allyl dextran 10K aldonic acid and the carboxylic functionalization. Matrix layers on the chip surfaces were finally prepared by simply soaking plasma-cleaned SPR gold chips in the surfactant solutions (0.1 mg/mL) overnight.

2.3.1. Synthesis of dextran aldonic acid

Dextran (3 g) in DI water (170 mL) was oxidized by 1 g of iodine and 0.9 g of potassium hydroxide for 24 h at room temperature. The unconsumed iodine was precipitated by means of silver carbonate. The solution was passed through a strong cationic exchange column (Amberlite IR-120) and dextran aldonic acid was recovered by lyophilization of the aqueous eluate to give ~2.2 g (~73%) of dextran aldonic acid. IR (KBr, cm^{-1}): 3440 (OH), 2925 (C—H), 1755

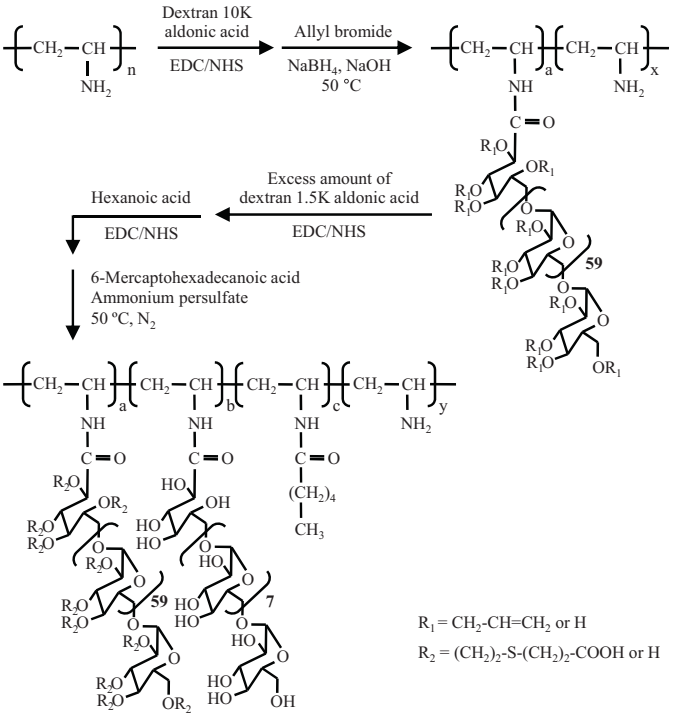

Scheme 1. Synthesis pathways to bimodal dextran surfactant polymer.

(C=O of COOH), 1650 (O—H of associated water) and 1200–1000 (C—O). ^{1}H NMR (D_2O, ppm): 3.2–4.0 (all CH and CH_2 except the ones at glycosidic linkages) and 4.85 (CH at glycosidic linkages).

2.3.2. Coupling of dextran 10K aldonic acid to PVAm (PVAm-g-dextran 10K)

Dextran 10K aldonic acid (8 and 30 mol% based on vinyl amine units) were fed to a 1 M sodium acetate buffer pH 4.5 (2 mL) containing 50 mg PVAm. EDC, NHS and MES were added at a fixed mole ratio of carboxyl group/EDC/NHS/MES (1:10:1:1) to the solution with magnetic stirring. After 24 h, the mixture was dialyzed against DI water (MWCO 14000 g/mol) and vacuum dried to obtain 346.2 mg (69%) and 747.8 mg (49%) of PVAm grafted with 8% and 30% dextran 10K aldonic acid, respectively. IR (KBr, cm^{-1}): 1643 (C=O of amide), 1559 (N—H of amine), and 1117 (C—O—C) and 1200–1000 (C—O of dextran). ^{1}H NMR (D_2O, ppm): 1.2–2.0 (CH_2 of PVAm and CH_3 of amine acetate), 3.2–4.0 (CH of PVAm and all CH and CH_2 except the ones at glycosidic linkages) and 4.85 (CH at glycosidic linkages).

2.3.3. Allylation of PVAm-g-dextran 10K (PVAm-g-allyl dextran 10K)

To an aq. solution (4 mL) of 30 mg PVAm-*g*-dextran 10K was added 7.4 mg of NaOH and 0.3 mg of sodium borohydride. Allyl bromide (0.32 mL) was added and the solution was stirred at 60 °C for 3 h. After neutralization with acetic acid, the mixture was dialyzed against DI water and dried to yield approximately 28 mg (~90%), regardless of grafting percentages of the dextran 10K aldonic acid. ^{1}H NMR (D_2O, ppm): 1.2–2.0 (CH_2 of PVAm), 3.2–4.0(CH of PVAm and all CH and CH_2 except the ones at glycosidic linkages), 4.1 (O—CH_2—C of allyl), 4.85 (CH at substituted glycosidic linkages) 5.0 (CH at non-substituted glycosidic linkages), 5.1–5.3 (CH_2—C of allyl) and 5.87 (C=CH—C of allyl).

2.3.4. Coupling of dextran aldonic acid and hexanoic acid

PVAm-*g*-allyl dextran 10K (10 mg) or pure PVAm (50 mg, for monomodal surfactant synthesis) was reacted with an excess amount of dextran 1.5K aldonic acid (100 mol% based on vinyl amine units) in a 1 M sodium acetate buffer pH 4.5 (4 mL). EDC (178 mg), NHS (27 mg) and MES (51 mg) were added to the solution with magnetic stirring. After 24 h, the solution was dialyzed against DI water and dried. The obtained PVAm-*g*-allyl dextran 10K/dextran 1.5K and PVAm-*g*-dextran 1.5K copolymers (10 mg) in 1 M sodium acetate buffer (4 mL) was sequentially capped with hexanoic acid (29 μL). EDC (178 mg), NHS (27 mg) and MES (51 mg) were added. After 24 h, the solution was dialyzed against DI water and dried. ^{1}H NMR (D_2O, ppm): 0.85 (CH_3 of hexanoyl groups), 1.2–2.1 (CH_2 of hexanyol groups and CH_2 of PVAm), 3.1–3.9 (CH of PVAm and all CH and CH_2 except the ones at glycosidic linkages), 4.1 (O—CH_2—C of allyl), 4.85 (CH at glycosidic linkages), 5.0–5.2 (CH_2=C of allyl) and 5.87 (C=CH—C of allyl).

2.3.5. Carboxylation of bimodal surfactant polymer

The allyl dextran surfactant polymer (5 mg) was reacted with 6-mercaptohexadecanoic acid (13 μL) in DMSO (4 mL) in the presence of ammonium persulfate (4 mg) at 50 °C under N_2 for 3 h. ^{1}H NMR (D_2O, ppm): 0.85 (CH_3 of hexanoyl groups), 1.2–2.1 (CH_2 of hexanyol groups and CH_2 of PVAm), 3.1–3.9 (CH of PVAm and all CH and CH_2 except the ones at glycosidic linkages) and 4.85 (CH at glycosidic linkages).

2.4. SPR experiments

A SPR imaging system built by the National Electronics and Computer Technology Center was employed. A light emitting diode light source makes a monochromatic light with 880 nm wavelength. A polarizer permits measurements both with p-polarized and s-polarized, being used as reference. A 1-inch gold chip for SPR measurement, purchased from Ssens (Hengelo, Netherland), was attached via an index matching oil to a prism on the SPR device, while the surfactant modified surface was equipped with a multichannel flow cell. A 10 mM HEPES buffered saline solution (HBS, pH 7.4) was utilized as a mobile phase.

An important viral shrimp pathogen, YHV, was selected as a model in this study. A standard inoculum, prepared as described previously, from a 1998 Thai YHV isolate (Sittidilokratna et al., 2002) was used to infect *Penaeus monodon*. Approximately 200 juvenile shrimps with an average weight of 20 g were infected by intramuscular injection with the inoculum. At 3 days post-infection, haemolymph was withdrawn and used as a source of virus for purification. As previously described, YHV was purified in an Urograffin (Schering, Berlin, Germany) density gradient by ultracentrifugation (Wongteerasupaya et al., 1995). The obtained purified YHV pellet was resuspended in TNE buffer (0.05 M Tris–HCl, 0.1 M NaCl, 1 mM EDTA, pH 7.4) and stored in aliquots at −80 °C.

A polyclonal antibody specific to the YHV envelope glycoprotein gp116 (Sittidilokratna et al., 2009) was generously provided by Dr. Paisarn Sithigorngul (Srinakha-rinwirot University, Thailand). The chip sensing surface was activated by a solution of EDC (0.2 M)/NHS (0.05 M)/MES (0.05 M). The antibody against the YHV (10 ng/mL) in 10 mM sodium acetate buffer (pH 4.5) was immobilized to the carboxylic groups of the high *MW* dextran side chains on the chip surface. After injection of ethanolamine solution (1 M), a shrimp virus solution (0.1 ng/mL) was passed over the ligand immobilized surface to record the SPR response at the end of the injection.

3. Results and discussion

Preliminary study of reversible self-assembling of the bimodal and monomodal dextran surfactant polymers has been previously reported briefly, but only contact angle measurement was presented (Sansatsadeekul & Mai-ngam, 2013). In this report, different

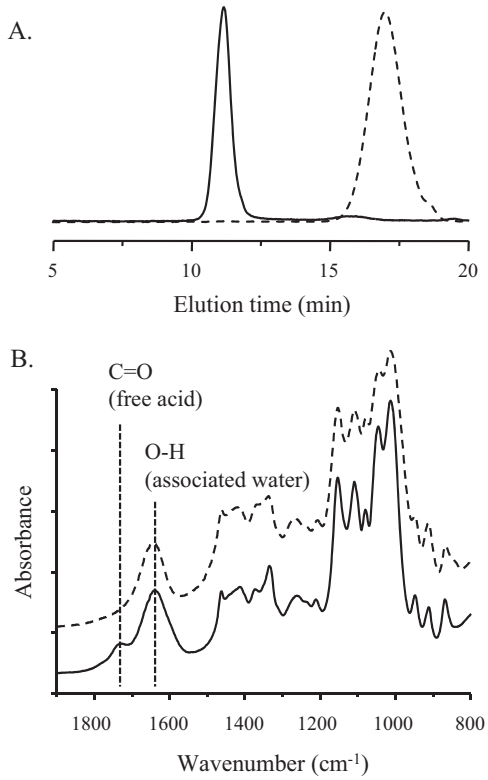

Fig. 1. GPC traces (A) and FT-IR spectra (B) of dextran 1.5K (dashed line) and the oxidation product of dextran 1.5K (solid line) after 24 h of reaction. GPC was carried out on a ultrahydrogel linear column using 0.1 M sodium nitrate buffer (pH 7) as eluent.

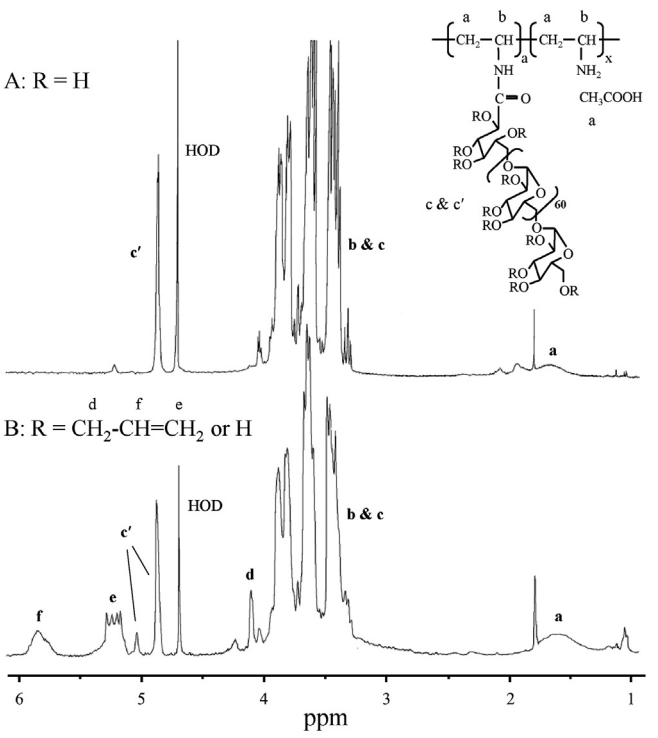

Fig. 2. ^{1}H NMR spectra of PVAm-*g*-dextran 10K (top) and PVAm-*g*-allyl dextran 10K (bottom) in D_2O where *a* and *x* are the mole percentages of dextran 10K and unreacted amino groups, respectively. Both spectra represent the graft copolymers obtained from 30 mol% of the dextran 10K in the feed.

characterization techniques were employed to better understand the chemical compositions of the surfactant polymers and their self-assembling arrangement on the SPR gold chip surface. The information was further used to explain the SPR detection results of virus.

3.1. Synthesis of bimodal and monomodal dextran surfactant polymers

Dextran aldonic acid was first synthesized by selective iodine-oxidation of its reducing end to carboxylic acid according to a well-established method with some modifications (Zhang & Marchant, 1994). An only subtle chemical difference between dextran and its oxidized product can lead to different chromatographic behavior. Incorporation of a carboxylic acid into the neutral dextran molecule decreased its retention time on a negatively charged Ultrahydrogel Linear GPC column (Waters Corp., USA) (Fig. 1A). A clear shift of the whole peak toward a shorter retention time was found, confirming its complete oxidation.

Lyophilization process converted dextran aldonic acid to dextran lactone. However, due to the fact that dextran aldonic acid is sensitive to the presence of water, it will easily hydrolyze back to its aldonic acid form in a tropical climate, with high humidity levels throughout the year. The expected carbonyl stretching peaks of δ-lactone and γ-lactone at 1745 and 1771 cm^{-1} were not found in all FTIR spectra of the lyophilized dextran aldonic acid (Fig. 1B) (Zhang & Marchant, 1994). Instead, a strong δ(O—H) peak of associated water at 1650 cm^{-1} (Park, 1971) and a shoulder peak at around 1755 cm^{-1} attributable to carbonyl stretching of the free acid were found.

PVAm-*g*-dextran 10K was prepared by reacting the amino groups of PVAm with dextran 10K aldonic acid via the activation reaction with EDC/NHS/MES system. The ^{1}H NMR spectrum of the PVAm-*g*-dextran 10K was recorded as shown in Fig. 2. The methylene groups in PVAm backbone and the methyl groups of the amine acetate appeared in a broad peak at 1.1–2.0 ppm. The characteristic peaks of protons in dextran appeared at two regions: at 4.85 ppm corresponding to H1 and at 3.2–4 ppm region corresponding to remaining protons, except three hydroxyl protons. Using the integrals of the protons at glycosidic linkages to the protons in the PVAm backbone in the PVAm-*g*-dextran 10K precursors, the molecular compositions of carboxyl dextran 10K in the final bimodal surfactant polymer products were estimated as shown in Table 1.

Some hydroxyl groups of dextran 10K side chains (~40% as evaluated with ^{1}H NMR) were converted to allyl groups by the treatment with allyl bromide. ^{1}H NMR spectrum of PVAm-*g*-allyl dextran 10K (Fig. 2B) showed three allylic protons of allyl groups ($-CH_2-CH=CH_2$) which appeared at 5.17, 5.25 and 5.85 ppm. The peak at 4.10 ppm was assigned to methylene proton ($-CH_2-$) in allyl group (Sun & Chu, 2006). The degree of allyl substitution was calculated as the *X*/*Y*, where *X* and *Y* are the integrated areas of the allyl methine protons ($\delta = 5.85$ ppm) and the H1 protons on dextran backbone ($\delta = 4.85$ ppm (substituted) and 5.1 ppm (non-substituted)), respectively.

After allylation, dextran 1.5K aldonic acid chains were sequentially attached to the PVAm-*g*-allyl dextran 10K using the EDC and NHS activation reaction in a MES buffer system (Scheme 1). The unreacted amine groups on the backbone were further grafted with hexanoic acid and the allyl groups on the dextran 10K were converted to carboxylic acid. Unfortunately, their NMR spectra become too complicated to be quantitatively analyzed.

The grafting degrees of both dextran 10K and 1.5K side chains in the final surfactant polymer products were estimated through C/N ratios of the products obtained from each grafting step (Table 1). To calculate the grafting composition, the increase in the C/N ratio after grafting was divided by the number of carbon atoms in each

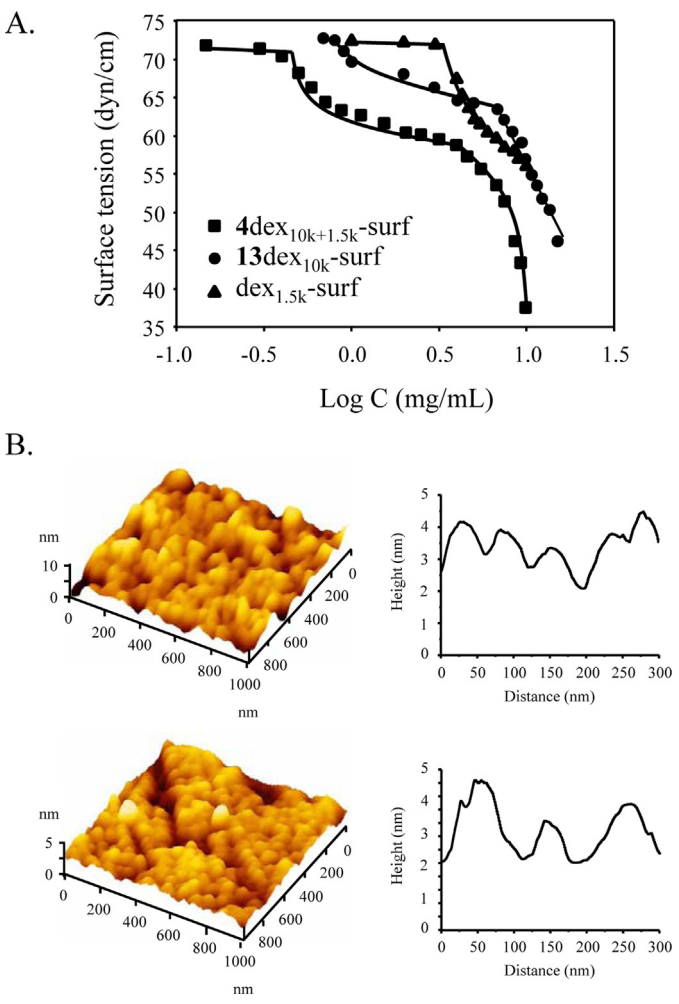

Fig. 3. (A) Plots of surface tension of aqueous solution vs. log concentration (mg/mL) for **4**dex$_{10k+1.5k}$ surf, **13**dex$_{10k}$ surf and dex$_{1.5k}$ surf at 25 °C. (B) AFM images and height profiles of a single surfactant matrix of **4**dex$_{10k+1.5k}$ (top) and a mixed surfactant matrix of **13**dex$_{10k}$/dex$_{1.5k}$ (bottom). The surfactant polymer adsorbed in aggregates with no order onto the gold chip surface.

dextran chain (54 atoms for dextran 1.5K and 336 atoms for dextran 10K). The actual percentages of dextran 10K for bimodal surfactant polymers synthesized from feed percentages of 8 and 30 (based on vinyl amine units) were determined to be 3.9 and 12.6 mol%, which were similar to those estimated from ^{1}H NMR. The surfactant polymers are designated as **4**dex$_{10k+1.5k}$-surf and **13**dex$_{10k}$-surf. The distance between their grafting points (d) on the **4**dex$_{10k+1.5k}$-surf is close to one and a half the radius of gyration of the unperturbed dextran 10K ($R_g \sim 3.4$ nm). In contrast, no gap between the densely grafted carboxyl dextran 10K side chains on the **13**dex$_{10k+1.5k}$-surf as it was found that the grafting distance is significantly less than R_g and dextran 1.5K aldonic acid chains could not be sequentially attached (Table 1). Note that the R_g of dextran was calculated using the empirical relation R_g (nm) = 0.066 × $Mw^{0.43}$ (Senti et al., 1955).

The monomodal surfactant polymer, PVAm with non-functionalized dextran 1.5K and hexyl branches (designated as dex$_{1.5k}$-surf), was also successfully synthesized. It was found that 24.1 mol% of its vinyl amine monomer units were grafted with dextran 1.5K.

The surface-active properties of the prepared dextran surfactant polymers at the air/water interface were obtained from surface tension measurements. The surface tension data were plotted against the logarithm of concentration (Fig. 3A). Note that the highest concentration employed for all tested dextran surfactant polymers was limited by their water solubility. All surfactants prepared could be used to effectively reduce water surface tension. They exhibit a substantial non-linear decrease in surface tension with increasing surfactant concentration. The lowest surface tension achieved is about 38 dyn/cm, a decrease of 34 dynes compared with pure water. No critical micelle phenomenon for all three surfactants was observed within the measured concentration range.

3.2. Matrix layer formation of non-covalently attached bimodal dextran

The layer formation of non-covalently 'end-on' attached dextran chains with bimodal molecular weight distributions on a SPR chip surface was investigated from the perspective of mixed physisorption of the prepared surfactant polymers. Six different matrix layers were prepared using surfactant mixture solutions with feed compositions shown in Table 2. As expected, mixing the monomodal dex$_{1.5k}$-surf to the bimodal **4**dex$_{10k+1.5k}$-surf solution resulted in a decrease in the surface density of the carboxyl dextran 10K side chains, as compared to that of the corresponding single surfactant matrix (Table 3). Moreover, the greater mixing percentages of the dex$_{1.5k}$-surf, the lower density of the carboxyl dextran 10K side chains.

Assembly of the surfactant polymers absorbed on gold chip surfaces was observed in AFM images in water and some examples of images and corresponding height profiles are shown in Fig. 3B. Note that those not shown here did not exhibit different topography. For both the mixed surfactant matrices and the single surfactant matrices, the surfactant adsorption was visualized as molecular aggregates, without enough hydrophobic force to drive the extension of PVAm backbone. The surfaces appear to be fully covered by surfactant molecules, which do not allow for direct height measurements by means of AFM.

If we assume that the dextran side chains adopt a spherical shape of the same density in water solution, the corresponding volumes, estimated from $4/3\pi(R_g)^3$, are approximately 174 nm^3 and 15 nm^3 for a carboxyl dextran10K and a dextran 1.5K, respectively. Moreover, if the presence of a PVAm backbone and hexyl side chains are neglected, the occupied volume and the lateral cross-section of the whole surfactant aggregate can be roughly estimated, as listed in Table 1. The lateral cross-sections of **4**dex$_{10k+1.5k}$-surf and **13**dex$_{10k}$-surf are calculated to be comparable (~70 nm), while that of the monomodal dex$_{1.5k}$-surf is less than half the value.

Height profile analysis was then performed from a series of AFM images to quantify the separation distances (D) between adsorbed aggregates (Table 3). The D values of both single surfactant matrices are approximately 60 nm, which is close to the calculated lateral cross-sections of **4**dex$_{10k+1.5k}$-surf and **13**dex$_{10k}$-surf. Therefore, we concluded that we were imaging **4**dex$_{10k+1.5k}$-surf and **13**dex$_{10k}$-surf aggregates.

As expected, the monomodal dex$_{1.5k}$-surf molecules acted as spacers between aggregates, which were evidenced from the greater separation distance between aggregates (D) with increasing the monomodal surfactant ratio. For the mixed matrices with the 1:1 ratio, the separation distance between aggregates (D) was calculated to be approximately 100 nm, which is expected for a lateral cross-section of a bimodal surfactant molecule combined with a monomodal surfactant molecule. However, the D value of the **6**dex$_{10k+1.5k}$/dex$_{1.5k}$ (1:3) didn't increase in the same proportion as the surfactant feed ratio.

For direct comparison, we prepared end-grafted bimodal dextran chips by sequentially reacting allyl dextran 10K aldonic acid (1 mg/mL) and non-functionalized dextran 1.5K aldonic acid (1 mg/mL) to an amine functionalized SPR gold chip directly via the EDC/NHS activation, prior to chemical modification of the allyl groups to carboxylic functional groups. The chips have been

Table 1
Compositions in the prepared dextran surfactant polymers.

	Bimodal surfactants		Monomodal surfactant
	4dex$_{10k+1.5k}$-surf	**13**dex$_{10k}$-surf	dex$_{1.5k}$-surf
Feed compositions (mol%)[a]			
Carboxylic dextran 10K	8	30	0
Dextran 1.5K	100	100	100
Compositions measured by ^{1}H NMR (mol%)[b]			
Carboxylic dextran 10K	4.4	11.5	0
C/N ratio of some intermediate products			
PVAm	2.48	2.48	2.48
PVAm-*g*-dextran 1.5k	–	–	15.51
PVAm-*g*-dextran 10K	16.87	48.52	–
PVAm-*g*-allyl dextran 10K	16.78	48.78	–
PVAm-*g*-ally dextran 10K /dextran 1.5K	28.67	48.23	–
Compositions estimated from C/N ratios (mol%)			
Carboxylic dextran 10K	3.9	12.6	0
Dextran 1.5K	22.0	0	24.1
Estimated number of groups per surfactant molecule[c]			
Carboxylic dextran 10K	92	300	0
Dextran 1.5K	522	0	572
Grafting distance between carboxylic dextran 10K (d, nm)[d]	6.5	2.0	n/a
Roughly estimated dimensions of a molecular aggregate[e]			
Occupied volume (nm^3)	24,000	52,000	2060
Lateral cross-section (nm)	60	75	25

[a] Calculated based on vinyl amine units.
[b] Estimated as the a/n value, where a = (integral of peak c')/62 (i.e., 62 protons from H1 of the dextran backbone) and n = {(integral of peak a) − 3a}/5 (i.e., 2 protons from —CH_2— of PVAm and 3 from CH_3 of the amine acetate).
[c] Estimated based on the average molar compositions and 2376 amino groups per PVAm molecule, estimated from its *MW*.
[d] Estimated as $d = (2376 \times 0.251)$/number of carboxylic dextran 10K per molecule, where the number of amino groups per PVAm molecule is 2376 and the length of each vinyl monomer is 0.251 nm.
[e] Estimated based on assumptions of a spherical volume and a negligible PVAm and hexyl.

Table 2
Feed compositions (%wt) of mixed surfactant polymers used to prepare non-covalently attached bimodal dextran matrices.

	4dex$_{10k+1.5k}$-surf	**13**dex$_{10k}$-surf	dex$_{1.5k}$-surf
Single surfactant matrices			
4dex$_{10k+1.5k}$	100	–	–
13dex$_{10k}$	–	100	–
Mixed surfactant matrices			
4dex$_{10k+1.5k}$/dex$_{1.5k}$ (6:1)	75	–	25
4dex$_{10k+1.5k}$/dex$_{1.5k}$ (1:1)	50	–	50
4dex$_{10k+1.5k}$/dex$_{1.5k}$ (1:3)	25	–	75
13dex$_{10k}$/dex$_{1.5k}$ (1:1)	–	50	50

Table 3
Surface densities of carboxyl dextran 10K in the different matrix layers and their SPR responses to the YHV solution (0.1 ng/mL).

	Density (nmol/m^2)[a]	Separation distance between aggregates (D, nm)[b]	Reflectivity change ($\Delta\%R_{YHV}$)[c]
Non-covalently attached matrices			
4dex$_{10k+1.5k}$	181.5	62.4 ± 16.8	0.97 ± 0.22
4dex$_{10k+1.5k}$/dex$_{1.5k}$ (3:1)	172.8	73.3 ± 16.5	6.07 ± 0.22
4d ex$_{10k+1.5k}$/dex$_{1.5k}$ (1:1)	155.6	100.0 ± 30.5	7.18 ± 0.21
4dex$_{10k+1.5k}$/dex$_{1.5k}$ (1:3)	80.7	121.6 ± 37.9	4.96 ± 0.25
13dex$_{10k}$	285.1	59.3 ± 4.1	0.85 ± 0.16
13dex$_{10k}$/dex$_{1.5k}$ (1:1)	262.9	96.3 ± 10.4	3.10 ± 0.04
Covalently grafted matrix[d]	99.7	n/a	0.41 ± 0.04

[a] Indirectly evaluated from surface carboxylic group density determined by TBO dye assay (Xu, Persson, Löfås, & Knoll, 2006) and an assumption that the allyl groups were completely converted to carboxylic acid.
[b] Estimated from the height profiles of the AFM images.
[c] The data are mean ± standard deviation.
[d] Prepared at a concentration of 1 mg/mL.

developed in our laboratory and effectively employed to assay various biomolecular species including proteins, antibodies and DNA, but no comparable success has been achieved for either viruses or bacteria. The end-grafted bimodal dextran chips consist of two major layers (inner and outer layers; Fig. 4A). The inner layer contains controlled ratios of short- and long-chain segments and provides polymeric repulsion against non-specific binding. The outer layer contains only long-chain segments with functional groups for ligand immobilization. The surface density of the carboxyl dextran10K chains was evaluated using TBO dye assay to be approximately 100 nmol/m^2 (Table 3). A single carboxyl dextran 10K molecule was estimated to cover a surface area of ~17 nm^2, corresponding to a lateral cross-section of ~4 nm. The separation distance between their neighboring molecules was slightly less than twice the radius of gyration of the dextran 10K, suggesting their full surface coverage. No effective reduction of the surface

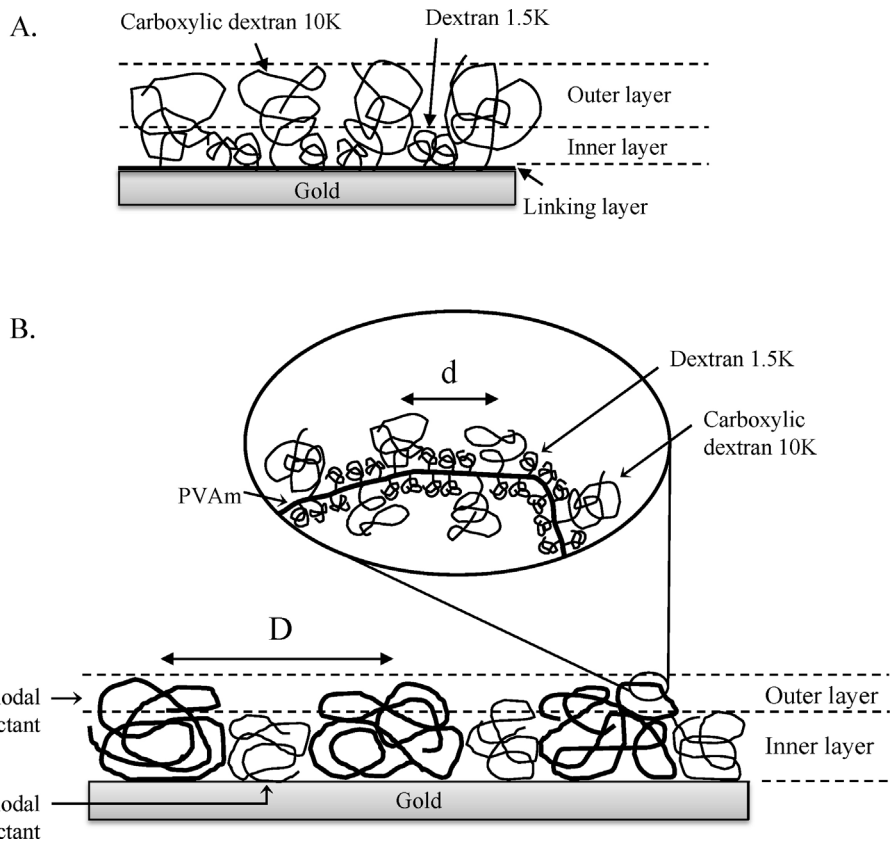

Fig. 4. Proposed models of (A) the directly end-grafted bimodal dextran and (B) the mixed surfactant **4**$dex_{10k+1.5k}/dex_{1.5k}$ matrix layer on SPR gold chips. Note that hexyl side chains are not shown in the mixed surfactant model and the scale ratio of *x*–*y* axis is ~1:5.

carboxylic dextran 10K density could be achieved through lowering the concentrations to 0.001 mg/mL (data not shown).

3.3. SPR analysis of virus detection on different bimodal dextran chips

Fig. 5 shows real-time sensorgrams obtained during antibody coupling and shrimp YHV detection. The physisorbed surfactant molecules stably remained on the surface as evidenced by a constant SPR response ($\Delta\%R_{anti\text{-}YHV} \sim 0.8\%$; dashed line) under flow conditions for the duration of virus detection. Table 3 also lists the SPR responses defined as the percentage of reflectivity changes to

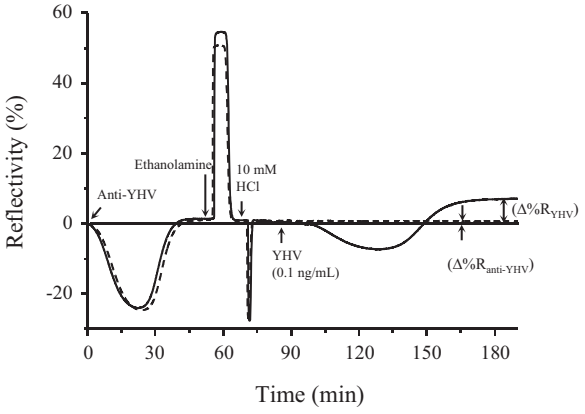

Fig. 5. Real-time sensorgrams from the **4**$dex_{10k+1.5k}/dex_{1.5k}$ (1:1) chip. The solid line shows covalent immobilization of anti-YHV followed with the YHV detection. The dashed line shows stability of the anti-YHV grafted surfactant polymer for the duration of experiment (no virus injection).

injection of shrimp YHV ($\Delta\%R_{YHV}$; solid line in Fig. 5) onto different bimodal dextran chips. A very weak SPR response to the YHV injection was found on the covalently end-grafted bimodal dextran chip. Greater values of $\Delta\%R_{YHV}$ were obtained for the non-covalently attached bimodal dextran chips generated by surfactant polymers and no correlation was found between the SPR response sensitivity and the different surface carboxylic dextran 10K densities of the surfactant polymers.

Fig. 4B shows a proposed model of the mixed surfactant $dex_{10k+1.5k}/dex_{1.5k}$ matrix layer on SPR gold chip based on the AFM data. We suspect that two molecular parameters are of importance in ligand–receptor bridge formation on the mixed surfactant chips: (a) a separation distance between the bimodal dextran surfactant aggregates, *D*, and (b) an intra-chain distance between the carboxyl dextran 10K side chains on the bimodal surfactant polymers, *d*. The non-functionalized monomodal surfactant molecules on the mixed surfactant chips acted as inter-chain spacer units (i.e., greater *D*) and consequently significantly enhanced the SPR sensitivity of YHV detection. Moreover, the mixed surfactant **13**$dex_{10k}/dex_{1.5k}$ matrix (larger *D*, lower *d*) exhibited a stronger response than the single surfactant **4**$dex_{10k+1.5k}$ matrix. Long range repulsion of highly hydrated polymers absorbed on a surface decay exponentially with distance, and this decay length depends linearly on its radius of gyration. This may explain the more pronounced efficiency of the separation distance between the bimodal surfactant aggregates to prevent viruses to approach ligands on the dextran 10K side chains, as compared to the intra-chain dextran 10K distance.

The strongest SPR response to YHV was found for the mixed surfactant **4**$dex_{10k+1.5k}/dex_{1.5k}$ (1:1) chip ($d = 6.5$ nm) and approximately two times greater than that of **13**$dex_{10k}/dex_{1.5k}$ (1:1) chip ($d = 2.0$ nm). Viruses may start to sense a local repulsion induced by the ligand linked dextran 10K side chains once they are

sufficiently close to each other. Additionally, clear spaces between the dextran 10K side chains (Fig. 4B, inset) allow more rod-shape YHV particles (40–50 × 150–170 nm) (Wongteerasupaya et al., 1995) to effectively approach the sensor chip surface within the capture distance where significant ligand–receptor bridge formation first occurred. However, the mixed surfactant **4**$dex_{10k+1.5k}$/$dex_{1.5k}$ (1:3) matrix layer with the relatively large separation distance between the antibody conjugated bimodal surfactant aggregates showed a weaker SPR response to the YHV solution as compared to the **4**$dex_{10k+1.5k}$/$dex_{1.5k}$ (1:1) chip, possibly due to its decreased probability to find binding sites of the approaching viruses.

4. Conclusion

Non-covalently 'end-on' attached bimodal dextran layers on SPR gold chip surfaces were generated by mixing two structurally well-defined surfactant polymers, including a bimodal carboxyl dextran surfactant polymer and a monomodal dextran surfactant polymer. A separation distance between the carboxyl dextran 10K side chains on the bimodal surfactant polymers could be controlled through the carboxyl dextran 10K composition in the bimodal surfactant polymer. A separation distance between the whole bimodal surfactant molecules on the chip surface depended on the mixing ratio of the two surfactant polymers. Synergetic adjustment of both separation distances allowed the relatively large rod-shape virus particles to effectively approach the sensor chip surface and form specific ligand–receptor bridges. This preliminary study provided encouraging results that demonstrate their potential to be successfully used in the future after optimization for different viruses.

Acknowledgments

This research project was financially supported by the National Electronic and Computer Technology Center, Thailand (P0900020). The SPR imaging instrument was lab-built by Dr. B. Sutapun and his team (National Electronic and Computer Technology Center, Thailand).

References

Bianco, A., Wu, W., Pastorin, G., Klumpp, C., Lacerda, L., Partidos, C. D., Kostarelos, K., & Prato, M. (2007). Carbon nanotube-based vectors for delivering immunotherapeutics and drugs. In *Nanotechnologies for the life sciences*. Weinheim: Wiley-VCH Verlag GmbH & Co. KGaA.

Bridgett, M. J., Davies, M. C., & Denyer, S. P. (1992). Control of staphylococcal adhesion to polystyrene surfaces by polymer surface modification with surfactants. *Biomaterials*, *13*(7), 411–416.

Helmus, M. N., & Hubbell, J. A. (1993). Materials selection. *Cardiovascular Pathology*, *2*(Suppl.), 53S–71S.

Holland, N. B., Qiu, Y., Ruegsegger, M., & Marchant, R. E. (1998). Biomimetic engineering of non-adhesive glycocalyx-like surfaces using oligosaccharide surfactant polymers. *Nature*, *392*(6678), 799–801.

Kam, N. W. S., Liu, Z., & Dai, H. (2005). Functionalization of carbon nanotubes via cleavable disulfide bonds for efficient intracellular delivery of siRNA and potent gene silencing. *Journal of the American Chemical Society*, *127*(36), 12492–12493.

Lahiri, J., Isaacs, L., Tien, J., & Whitesides, G. M. (1999). A strategy for the generation of surfaces presenting ligands for studies of binding based on an active ester as a common reactive intermediate: A surface plasmon resonance study. *Analytical Chemistry*, *71*(4), 777–790.

Lei, Y., Chen, H., Dai, H., Zeng, Z., Lin, Y., Zhou, F., & Pang, D. (2008). Electroless-plated gold films for sensitive surface plasmon resonance detection of white spot syndrome virus. *Biosensors and Bioelectronics*, *23*(7), 1200–1207.

Löfås, S., & McWhirter, A. (2006). The art of immobilization for SPR sensors. In J. Homola (Ed.), *Surface plasmon resonance based sensors* (vol. 4) (pp. 117–151). Berlin, Heidelberg: Springer.

Mai-ngam, K. (2006). Comblike poly(ethylene oxide)/hydrophobic C6 branched chitosan surfactant polymers as anti-infection surface modifying agents. *Colloids and Surfaces B: Biointerfaces*, *49*(2), 117–125.

Marsh, L. H., Coke, M., Dettmar, P. W., Ewen, R. J., Havler, M., Nevell, T. G., Smart, J. D., Smith, J. R., Timmins, B., Tsibouklis, J., & Alexander, C. (2002). Adsorbed poly(ethyleneoxide)-poly(propyleneoxide) copolymers on synthetic surfaces: Spectroscopy and microscopy of polymer structures and effects on adhesion of skin-borne bacteria. *Journal of Biomedical Materials Research*, *61*(4), 641–652.

Park, F. S. (1971). Carbohydrates. In *Application of IR spectroscopy in biochemistry, biology, and medicine*. New York, NY: Plenum Press.

Park, J. H., Cho, Y. W., Kwon, I. C., Jeong, S. Y., & Bae, Y. H. (2002). Assessment of PEO/PTMO multiblock copolymer/segmented polyurethane blends as coating materials for urinary catheters: In vitro bacterial adhesion and encrustation behavior. *Biomaterials*, *23*(19), 3991–4000.

Puttharugsa, C., Wangkam, T., Huangkamhang, N., Gajanandana, O., Himananto, O., Sutapun, B., Amarit, R., Somboonkaew, A., & Srikhirin, T. (2011). Development of surface plasmon resonance imaging for detection of *Acidovorax avenae* subsp. *citrulli* (Aac) using specific monoclonal antibody. *Biosensors and Bioelectronics*, *26*(5), 2341–2346.

Qiu, Y., Zhang, T., Ruegsegger, M., & Marchant, R. E. (1998). Novel nonionic oligosaccharide surfactant polymers derived from poly(vinylamine) with pendant dextran and hexanoyl groups. *Macromolecules*, *31*(1), 165–171.

Richens, J., Urbanowicz, R., Lunt, E., Metcalf, R., Corne, J., Fairclough, L., & O'Shea, P. (2009). Systems biology coupled with label-free high-throughput detection as a novel approach for diagnosis of chronic obstructive pulmonary disease. *Respiratory Research*, *10*(1), 29.

Ruegsegger, M. A., & Marchant, R. E. (2001). Reduced protein adsorption and platelet adhesion by controlled variation of oligomaltose surfactant polymer coatings. *Journal of Biomedical Materials Research*, *56*(2), 159–167.

Sagnella, S., & Mai-Ngam, K. (2005). Chitosan based surfactant polymers designed to improve blood compatibility on biomaterials. *Colloids and Surfaces B: Biointerfaces*, *42*(2), 147–155.

Sansatsadeekul, J., & Mai-ngam, K. (2013). Reversible self-assembling of comb-like functionalized dextran surfactant polymers as an SPR-sensing surfaces. *Advanced Materials Research*, *747*, 225–229.

Sen Gupta, A., Wang, S., Link, E., Anderson, E. H., Hofmann, C., Lewandowski, J., Kottke-Marchant, K., & Marchant, R. E. (2006). Glycocalyx-mimetic dextran-modified poly(vinyl amine) surfactant coating reduces platelet adhesion on medical-grade polycarbonate surface. *Biomaterials*, *27*(16), 3084–3095.

Senti, F. R., Hellman, N. N., Ludwig, N. H., Babcock, G. E., Tobin, R., Glass, C. A., & Lamberts, B. L. (1955). Viscosity, sedimentation, and light-scattering properties of fraction of an acid-hydrolyzed dextran. *Journal of Polymer Science*, *17*, 527–546.

Sittidilokratna, N., Chotwiwatthanakun, C., Wijegoonawardane, P. K. M., Unajak, S., Boonnad, A., Wangnai, W., Jitrapakdee, S., Cowley, J. A., & Walker, P. J. (2009). A virulent isolate of yellow head nidovirus contains a deformed envelope glycoprotein gp116. *Virology*, *384*(1), 192–200.

Sittidilokratna, N., Hodgson, R. A. J., Cowley, J. A., Jitrapakdee, S., Boonsaeng, V., Panyim, S., & Walker, P. J. (2002). Complete ORF1b-gene sequence indicates yellow head virus is an invertebrate nidovirus. *Diseases of Aquatic Organisms*, *50*(2), 87–93.

Sun, G., & Chu, C.-C. (2006). Synthesis, characterization of biodegradable dextran–allyl isocyanate–ethylamine/polyethylene glycol–diacrylate hydrogels and their in vitro release of albumin. *Carbohydrate Polymers*, *65*(3), 273–287.

Vacheethasanee, K., & Marchant, R. E. (2000). Surfactant polymers designed to suppress bacterial (*Staphylococcus epidermidis*) adhesion on biomaterials. *Journal of Biomedical Materials Research*, *50*(3), 302–312.

Wongteerasupaya, C., Sriurairatana, S., Vickers, J. E., Akrajamorn, A., Boonsaeng, V., Panyim, S., Tassanakajon, A., Withyachumnarnkul, B., & Flegel, T. W. (1995). Yellow head virus of *Penaeus monodon* is an RNA virus. *Diseases of Aquatic Organisms*, *22*, 45–50.

Xu, F., Persson, B., Löfås, S., & Knoll, W. (2006). Surface plasmon optical studies of carboxymethyl dextran brushes versus networks. *Langmuir*, *22*(7), 3352–3357.

Zhang, T., & Marchant, R. E. (1994). Novel polysaccharide surfactants: Synthesis of model compounds and dextran-based surfactants. *Macromolecules*, *27*(25), 7302–7308.

Zhu, J., & Marchant, R. E. (2006). Dendritic saccharide surfactant polymers as antifouling interface materials to reduce platelet adhesion. *Biomacromolecules*, *7*(4), 1036–1041.